Journal of Power Sources 185 (2008) 1201–1208

Contents lists available at ScienceDirect

Journal of Power Sources

journal homepage: www.elsevier.com/locate/jpowsour

Modeling of a 5-cell direct methanol fuel cell using adaptive-network-based fuzzy inference systems

Rongrong Wang[a], Liang Qi[b], Xiaofeng Xie[b,*], Qingqing Ding[c], Chunwen Li[a,**], ChenChi M. Ma[d]

[a] Department of Automation, Tsinghua University, Beijing 100084, China
[b] Institute of Nuclear and New Energy Technology, Tsinghua University, Beijing 100084, China
[c] Department of Electrical Engineering, Tsinghua University, Beijing 100084, China
[d] National Tsing Hua University, Hsinchu 300, Taiwan

ARTICLE INFO

Article history:
Received 8 May 2008
Received in revised form 27 June 2008
Accepted 27 June 2008
Available online 15 July 2008

Keywords:
Direct methanol fuel cell (DMFC)
Adaptive-network-based fuzzy inference system (ANFIS)
Artificial neural network (ANN)
Polynomial-based model
Modeling

ABSTRACT

The methanol concentrations, temperature and current were considered as inputs, the cell voltage was taken as output, and the performance of a direct methanol fuel cell (DMFC) was modeled by adaptive-network-based fuzzy inference systems (ANFIS). The artificial neural network (ANN) and polynomial-based models were selected to be compared with the ANFIS in respect of quality and accuracy. Based on the ANFIS model obtained, the characteristics of the DMFC were studied. The results show that temperature and methanol concentration greatly affect the performance of the DMFC. Within a restricted current range, the methanol concentration does not greatly affect the stack voltage. In order to obtain higher fuel utilization efficiency, the methanol concentrations and temperatures should be adjusted according to the load on the system.

1. Introduction

Direct methanol fuel cells (DMFCs) are one of the most promising energy conversion devices for portable applications due to their high energy density for the generation of electric power from fuel [1]. The output voltage of the DMFC is affected by many factors such as air flow rates, temperature and methanol concentration [2–4]. In order to overcome these problems, it is necessary to find a simplified model to design a control strategy for the DMFC system.

The precise mathematical models are of great importance for feasibility studies and optimization of the DMFC system. However, it is very difficult to build up an analytical model due to the complex nonlinear multi-input and multi-output characteristics for the DMFC system [5]. Although many physical models have been presented so far, most of them focus on the design of the DMFC and description of the relevant internal details [6–8]. In fact, many users greatly need models that can describe the behavior of fuel cells under various operating conditions. Such models are, at the very least, important for research into the control of fuel cells.

The artificial neural network (ANN) has been accepted as an effective modeling method and can be used to capture complex input/output relationships of interest [9,10]. The fuzzy inference system (FIS) can model the qualitative aspects of human knowledge and the reasoning processes without precise quantitative analyses. It is well suited for dealing with ill-defined and uncertain systems [11]. A hybrid of ANN and FIS can make use of the advantages of both ANN and FIS, and it has become one focus of research in recent years [12–14]. A specific approach in a hybrid of ANN and FIS development is the adaptive-network-based fuzzy inference system (ANFIS), which serves as a basis for constructing a set of fuzzy rules with appropriate functions to generate the stipulated input/output pairs [15]. The ANFIS approach has recently been recognized as an effective modeling method in many fields of engineering [16–18]. Entchev and Wu successfully used ANFIS to model the solid oxide fuel cell (SOFC) [16,19]. Tao and Dong devised thermal models for proton exchange membrane fuel cells (PEMFCs) based on ANFIS [17,20]. To our best knowledge, however, no published papers have used ANFIS to model the performance of DMFC or PEMFC with multi-inputs.

In this study, the concept of ANFIS, ANN- and polynomial-based models are described. The temperature, current and methanol concentrations were taken as inputs, the cell voltage was taken as output, and the cell performance was identified by ANFIS. The ANN- and polynomial-based model were selected to be compared with

* Corresponding author at: A316, INET, Tsinghua University, Beijing 100084, China. Tel.: +86 10 62784827; fax: +86 10 62771150.
** Corresponding author. Tel.: +86 10 62799024; fax: +86 10 62795356.
E-mail addresses: xiexf@tsinghua.edu.cn (X. Xie), lcw@tsinghua.edu.cn (C. Li).

0378-7753/$ – see front matter © 2008 Published by Elsevier B.V.
doi:10.1016/j.jpowsour.2008.06.090

Nomenclature

a	coefficient of polynomial model
$\tilde{a}$	coefficient vector of polynomial model
b_i	bias for the ith neuron in the hidden layer of ANN
C	methanol concentration
CC	correlation coefficient
CCS	constant concentration surface
Cov	covariance
d	slope parameter of sigmoid function
D	variance
E	reversible open-circuit voltage (V)
FIS	fuzzy inference system
g	sigmoid function
I	current (A)
m	actual cell voltage from experiment
M	vectors made up of actual experimental values
MF	membership function
N	number of data points
p	predicted value by models
P	vectors made up of predicted values by models
R	correlation coefficient
RMSE	root mean square error
S	parameter set of ANFIS
S_1	premise set of ANFIS
S_2	consequent set of ANFIS
T	absolute temperature (K)
u	firing strength of a rule in the ANFIS
v	hidden layer input of the ANN
V	stack output voltage (V)
$\tilde{V}$	vector made up of stack voltage at various condition
w_{ij}	weight from the jth input to the ith hidden layer neuron in ANN
w^o_{ki}	weight from the ith output in the hidden layer to the kth output layer neuron in ANN
y_k	output from the kth output neuron of ANN
z	output of ANFIS

Greek symbol

μ	membership function of ANFIS

the ANFIS in respect of quality and accuracy. The results show that the ANFIS-based model has a better performance than the ANN- and polynomial-based models.

2. Experiments and samples

2.1. Experiment

The membrane electrode assembly (MEA) consisted of a polymer membrane, the anode and the cathode catalyst layers and two gas diffusion layers. Nafion117 (DuPont®) was used as a membrane. Each cell has an active area of 48.2 cm^2. The stack was assembled using a homemade housing which comprised two epoxy resin end plates and two copper plates of 3 mm thickness as current collectors. A picture of the DMFC stack is shown in Fig. 1.

The test system consisted of an electronic load controller, a methanol solution tank, a heat exchanger, a water bath for pre-heating the methanol solution, a gear pump for pumping methanol solution, an air compressor and an Ethernet Multimeter/data logger system for logging measurements. All experimental data were obtained at ambient pressure. Details of the cell and test system can be found elsewhere [21].

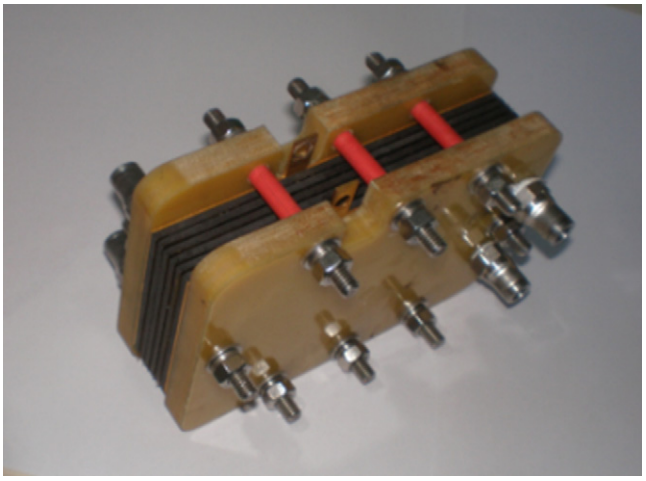

Fig. 1. Photograph of the tested 5-cell DMFC stack.

2.2. Preparation of data sets

The methanol solution was pre-heated to the desired temperature before it was delivered to the fuel cell stack. The flow rates of air and methanol solution were kept constant. The methanol exhausting from the testing stack was not allowed to circulate back to the solution tank in order to keep the methanol concentration constant.

A typical I–V characteristic of the DMFC is shown in Fig. 2. It shows that there is a large voltage drop at low current densities (i.e., close to the open-circuit voltage, OCV). This region is known as the activation polarization region. Modeling with data set taken from within the activation polarization region will make the performance of the model worse due to the rapid change of voltage. It is not necessary to model the fuel cell condition in this region because the current is too small.

In this study, six methanol concentrations from 0.67 to 2.33 mol L^{-1} (increments of 0.33 mol L^{-1}) were tested. Each of the six levels was assigned with sufficient measurement points in the temperature range from 25 to 55 °C and the voltage range from 1.3 to 3 V. The data set was separated into training data and checking data at a ratio of 3:1. The training data set was used to train the models, whereas the checking data set was used to verify the effectiveness of the models obtained. The checking points were selected at random from the whole data base. The distribution of the 1 mol L^{-1}

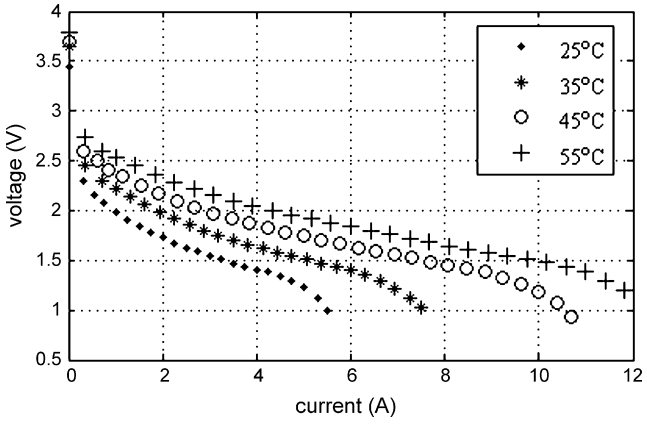

Fig. 2. I–V characteristics of the DMFC stack (methanol concentration, 1.00 mol L^{-1}).

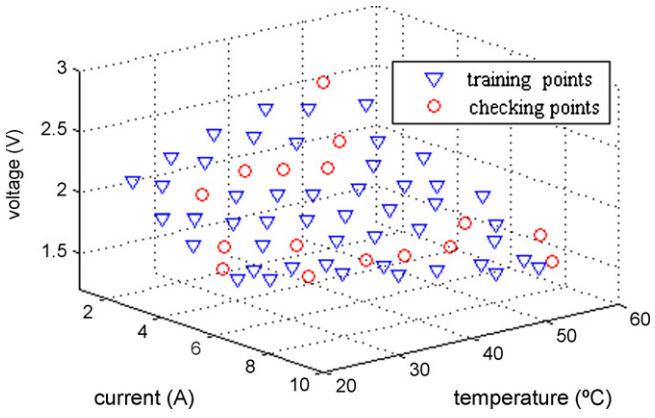

Fig. 3. The distribution of the checking and training points in the three-dimensional measurement space (methanol concentration, 1.00 mol L^{-1}).

Table 1
The number of training and checking points at each concentration

Concentration (mol L^{-1})	Number of training points	Number of checking points
0.67	45	15
1.00	48	16
1.33	40	13
1.67	42	15
2.00	56	18
2.33	54	18

level training and checking points in the three-dimensional measurement space is shown in Fig. 3. The number of training points and checking points for each concentration are listed in Table 1.

3. Method formulation

3.1. Polynomial-based models

The voltage of a DMFC depends very much on the operating conditions including temperature, methanol concentration and the flow rates of air and methanol solution [22]. When the flow rates of methanol and air are kept constant, the voltage can be written as [23]:

$$V = h(I, C, T) \tag{1}$$

where C denotes the methanol concentration and V, I and T denote the theoretical open-circuit voltage, voltage and current, respectively. The function in Eq. (1) can be approximated as follows [23]:

$$\begin{aligned} V = h(I, C, T) = {} & a_1 + a_2 I + a_3 C + a_4 T + a_5 IC + a_6 IT + a_7 CT + a_8 I^2 \\ & + a_9 C^2 + a_{10} T^2 + a_{11} ICT + a_{12} I^2 C + a_{13} I^2 T \\ & + a_{14} C^2 T + \cdots + a_n I^s C^p T^q \end{aligned} \tag{2}$$

where $\vec{a} = [a_1, a_2, \ldots, a_n]^{\mathrm{T}}$ are the unknown constant coefficients to be determined and the subscript n of a_n denotes the number of unknown coefficients.

In order to solve $\vec{a}$, different experimental measurements [I_i, C_i, T_i] with $i = 1, 2, \ldots, m$ are taken for various current, concentrations and temperature. These are substituted into Eq. (2) to produce a set of polynomial equations:

$$\vec{h} = \begin{bmatrix} V_1 \\ V_2 \\ \vdots \\ V_m \end{bmatrix} = \begin{bmatrix} 1 & I_1 & C_1 & T_1 & I_1C_1 & I_1T_1 & C_1T_1 & {I_1}^2 & {C_1}^2 & {T_1}^2 & I_1C_1T_1 & \cdots & I_1^s C_1^p T_1^q \\ 1 & I_2 & C_2 & T_2 & I_2C_2 & I_2T_2 & C_2T_2 & {I_2}^2 & {C_2}^2 & {T_2}^2 & I_2C_2T_2 & \cdots & I_2^s C_2^p T_2^q \\ \vdots & \vdots & \vdots & \vdots & \vdots & \vdots & \vdots & \vdots & \vdots & \vdots & \vdots & \vdots & \vdots \\ 1 & I_m & C_m & T_m & I_mC_m & I_mT_m & C_mT_m & {I_m}^2 & {C_m}^2 & {T_m}^2 & I_mC_mT_m & \cdots & I_m^s C_m^p T_m^q \end{bmatrix} \begin{bmatrix} a_1 \\ a_2 \\ \vdots \\ a_n \end{bmatrix} \Rightarrow \vec{V} = Q\vec{a}$$

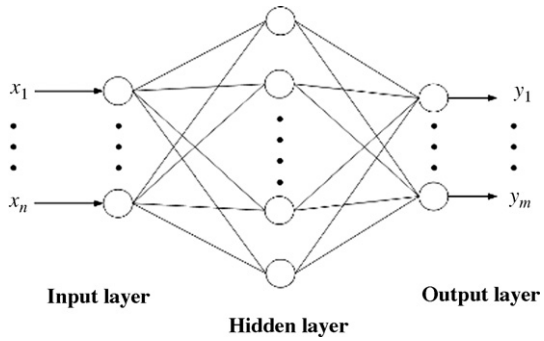

Fig. 4. Structure of a feed-forward three-layer neural network.

Therefore, the unknown coefficients $\vec{a} = [a_1, a_2, \ldots, a_n]^{\mathrm{T}}$ can be solved by the least-squares method (LSM) [23] as follows:

$$\vec{a} = (Q^{\mathrm{T}}Q)^{-1}Q^{\mathrm{T}}\vec{V} \tag{4}$$

3.2. Artificial neural network (ANN)

ANN can approximate any linear or nonlinear function well. A feed-forward neural network with supervised training [24] was utilized in this study. The structure of the feed-forward three-layer neural network is shown in Fig. 4.

The network consists of an input layer, a hidden layer and an output layer. The transfer function for the hidden layer is a sigmoid function, whose form is defined by:

$$g(v) = \frac{1}{1 + \mathrm{e}^{-dv}} \tag{5}$$

where d is the slope parameter. The input of the hidden layer can be described by the following equation:

$$v_i = \sum_{j=1}^{n} w_{ij} x_j + b_i \tag{6}$$

where w_{ij} is the weight from the jth input x_j to the ith neuron in the hidden layer, and b_i is the bias. If the function in the output layer is linear, the model equation for the entire network can be expressed as follows:

$$y_k = \sum_{i=1}^{N} w_{ki}^{o} v_i = \sum_{i=1}^{N} w_{ki}^{o} g\left(\sum_{j=1}^{n} w_{ij} x_j + b_i\right) \tag{7}$$

where y_k is the output signal from the kth output neuron, and w_{ki}^{o} is the weight from the ith output v_i to the kth neuron in the output layer. In this study, the weights and bias values of ANN are updated according to the gradient descent momentum algorithm, which is considered to be one of the best training algorithms for the ANN.

3.3. Adaptive-network-based fuzzy inference system

The ANFIS is a 5-layered network, in which the layers are not fully connected and the membership function parameters are extracted from a data set that describes the system behavior. The ANFIS learns features in the data set and adjusts the system parameters according to the given error criterion.

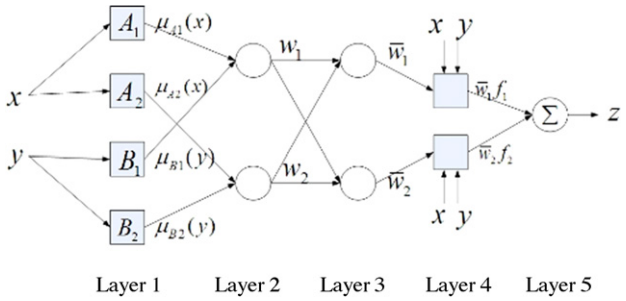

Fig. 5. Structure of an adaptive neuro-fuzzy inference system.

For simplicity, suppose that the ANFIS under consideration has two inputs and one output, and that the rule base for the system contains just two fuzzy if-then rules of the Takagi and Sugeno type [25].

(1) *Rule 1*: if x is A_1 and y is B_1, then $z_1 = p_1x + q_1y + r_1$.
(2) *Rule 2*: if x is A_2 and y is B_2, then $z_2 = p_2x + q_2y + r_2$.

where A and B are known as the linguistic labels. The ANFIS architecture is shown in Fig. 5, in which a circle indicates a fixed node and a square indicates an adaptive node. The node functions in the same layer are of the same function family as described below:

Layer 1: In this layer the functions of the nodes should be bell-shaped with a maximum value equal to 1 and minimum to 0. The functions used were:

$$\mu_{A_i}(x) = \frac{1}{1 + |(x - c_i)/a_i|^{2b_i}}, \quad i = 1, 2, \tag{8}$$

$$\mu_{B_j}(y) = \frac{1}{1 + |(y - c_j)/a_j|^{2b_j}}, \quad j = 1, 2, \tag{9}$$

where $\mu_{A_i}(x)$ and $\mu_{B_j}(y)$ are the membership functions (MFs) with the parameter set $\{a_i, b_i, c_i\}$. As the values of these parameters change, the bell-shaped functions vary accordingly.

Layer 2: Every node in this layer multiplies all the incoming signals (the output of first layer) and sends out the product.

$$u_i = \mu_{A_i}(x) \times \mu_{B_j}(y), \quad i = 1, 2, \quad \text{and} \quad j = 1, 2, \tag{10}$$

Each node output represents the firing strength of a rule.

Layer 3: The ith node in the layer calculates the ratio of the ith rule's firing strength to the sum of all rules firing strength.

$$\bar{u}_i = \frac{u_i}{u_1 + u_2}, \quad i = 1, 2, \tag{11}$$

where u_1 and u_2 are the outputs of the two nodes of the second layer.

Layer 4: The dimension of the layer determines the number of fuzzy rules in the system. Every node in this layer is a square node with a linear function whose form is defined by

$$O_i^4 = \bar{u}_i z_i = \bar{u}_i(p_i x + q_i y + r_i), \quad i = 1, 2, \tag{12}$$

where $\bar{u}_i$ is the output of layer 3, and $\{p_i, q_i, r_i\}$ denotes the parameter set referred to as the consequent parameters.

Layer 5: The single node in the layer simply computes the sum of the layer 4 outputs in order to obtain the overall system output, i.e.,

$$z = \sum_i \bar{u}_i z_i = \bar{u}_1 z_1 + \bar{u}_2 z_2 = \frac{u_1}{u_1 + u_2} z_1 + \frac{u_2}{u_1 + u_2} z_2 \tag{13}$$

The ANFIS network should be trained to learn about the data and its nature. During the learning processes, the parameters were tuned until the desired output was reached. The gradient descent method can be used to identify the parameters in the ANFIS. However, the gradient descent method is slow and tends to be trapped in local minima. Therefore, a hybrid learning algorithm was used to identify the parameters of ANFIS. It applied a combination of the LSM and the back-propagation gradient descent method for training FIS membership function parameters to emulate a given training data set.

The parameter set S in the proposed network can be spilt into two subsets:

$$S = S_1 \oplus S_2 \tag{14}$$

where $\oplus$ is the direct sum, and S_1 and S_2 represent premise and consequent sets, respectively. In fact, since the network output is obtained as a linear combination of all coming signals, the output z can be described as:

$$z = (\bar{u}_1 x)p_1 + (\bar{u}_1 y)q_1 + \bar{u}_1 r_1 + (\bar{u}_2 x)p_2 + (\bar{u}_2 y)q_2 + \bar{u}_2 r_2 \tag{15}$$

The learning rules are performed through two steps: the consequent parameters are first identified by the LSM, and then the error rates propagate backward and the premise is updated by the gradient descent method [15].

3.4. Criteria for performance evaluation

The performance of the models can be evaluated using different criteria. In this work, the performance of each model was evaluated by the root mean square error (RMSE) and correlation coefficients (CC) for the training and testing data sets.

The RMSE is defined by:

$$\text{RMSE} = \sqrt{\frac{1}{N}\sum_{i=1}^{N}(p_i - m_i)^2} \tag{16}$$

where m is the actual value from experiments, p is the predicted value from the models and N is the number of data points.

The CC is defined by:

$$R = \frac{\text{Cov}(M, P)}{\sqrt{\text{D}(M)}\sqrt{\text{D}(P)}} \tag{17}$$

where M and P are vectors made up of the actual value from experiments and the predicted value from models, respectively. Cov(M,P) is the covariance for vectors M and P, where D(M) and D(P) denote the variance of M and P, respectively. The closer the correlation coefficient R is to 1, the more precise is the model.

4. Results and discussion

In order to compare the performance of the different modeling methods, the models were trained with the same training data set. The validity of the models obtained was tested using the same checking data set. The CC of the checking data and the RMSE of training and checking data for each model are listed in Table 2.

4.1. Comparison of modeling accuracy

Fig. 6 shows the results of the polynomial models compared with the 95 checking data points. Third-order, forth-order and fifth-order polynomials with 20, 35 and 56 unknown constant coefficients, respectively, were trained and checked. It was found that the fifth-order polynomial had the best performance due to the largest coefficient number. Sixth-order polynomial was also tried out in this study, but it was found that the generalization capability was very bad as the RMSE for the checking data was abnormally large.

Table 2
Modeling results with different types of models

Models	RMSE (training data)	RMSE (checking data)	Correlation coefficient (checking data)
Polynomial (third-order)	0.03743	0.05033	0.99570
Polynomial (forth-order)	0.03596	0.04777	0.99651
Polynomial (fifth-order)	0.03382	0.04373	0.99757
ANN (10 hidden nodes)	0.02371	0.03955	0.99838
ANN (15 hidden nodes)	0.02188	0.03619	0.99835
ANN (20 hidden nodes)	0.02124	0.03520	0.99900
ANN (25 hidden nodes)	0.01920	0.03725	0.99874
ANN (30 hidden nodes)	0.01906	0.04428	0.99851
ANFIS (2-2-2)	0.03460	0.04597	0.99709
ANFIS (3-2-2)	0.02283	0.03571	0.99873
ANFIS (2-3-2)	0.03282	0.04769	0.99662
ANFIS (2-2-3)	0.03361	0.04797	0.99656
ANFIS (3-3-2)	0.02049	0.03120	0.99907
ANFIS (3-2-3)	0.01819	0.03380	0.99804
ANFIS (2-3-3)	0.03268	0.04889	0.99639
ANFIS (3-3-3)	0.01753	0.03565	0.99892
ANFIS (4-3-3)	0.01781	0.03031	0.99933
ANFIS (3-4-3)	0.01646	0.04153	0.99805
ANFIS (3-3-4)	0.01528	0.06499	0.99194
ANFIS (4-4-3)	0.01874	0.03860	0.99851
ANFIS (4-3-4)	0.01693	0.06289	0.99185
ANFIS (3-4-4)	0.01616	0.06274	0.99183
ANFIS (4-4-4)	0.01520	0.07963	0.98013

Fig. 7 shows the predicted values of the ANN-based models compared with the checking data points. During the early stage of the training, the checking error decreased rapidly. Over-fitting was recognized by the error becoming flat or even increasing slightly, and at this point the training was stopped. Many better ANN models with different numbers of hidden nodes were trained. It was found that the greater the number of hidden nodes, the smaller was the RMSE for the training data, that is the ANN with more hidden nodes could approximate the training data more precisely. However, too many hidden nodes might lead to over-fitting on the experimental data and a decreased generalization capability of the ANN. For example, the checking RMSE of the ANN with 20 and 30 hidden nodes were 0.03520 and 0.04428, respectively. This means that the ANN with 20 hidden nodes has better generalization capability than that of the ANN with 30 hidden nodes.

Comparison of predicted values of 95 checking data points using two ANFIS-based models, is shown in Fig. 8. ANFIS with different types of MFs such as triangular-shaped, Gaussian curve, Sigmoid-shaped MFs and the like [26] were tried out. Among these different types of MFs, the Gaussian curve MF provided the best results for

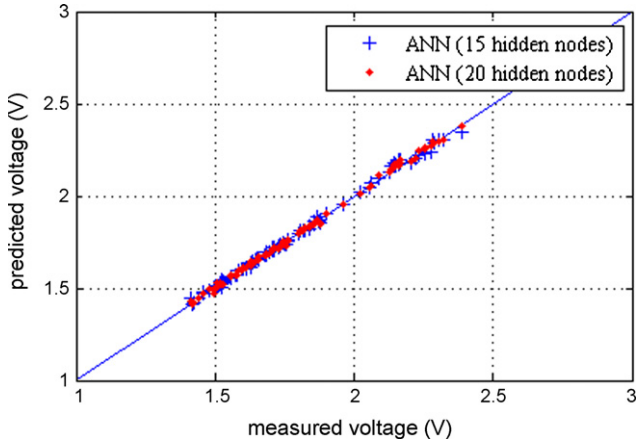

Fig. 7. Comparison of the predicted cell voltage using the ANN-based models with actual experimental values.

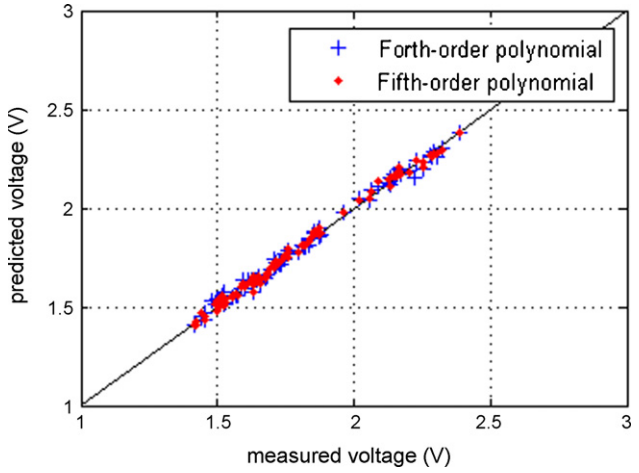

Fig. 6. Comparison of the predicted cell voltage using the polynomial-based model with actual experimental values.

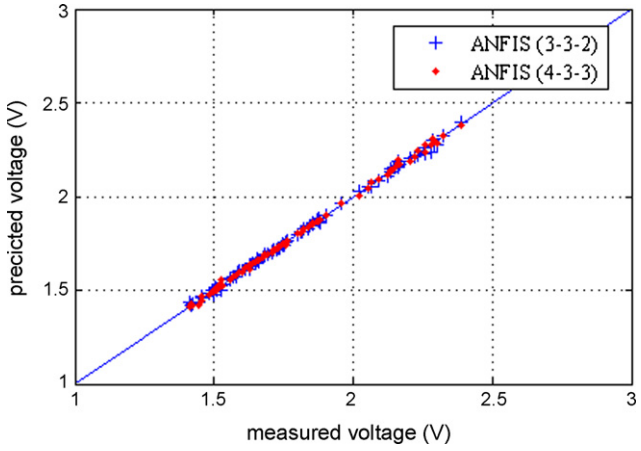

Fig. 8. Comparison of the predicted cell voltage using the ANFIS-based models with actual experimental values.

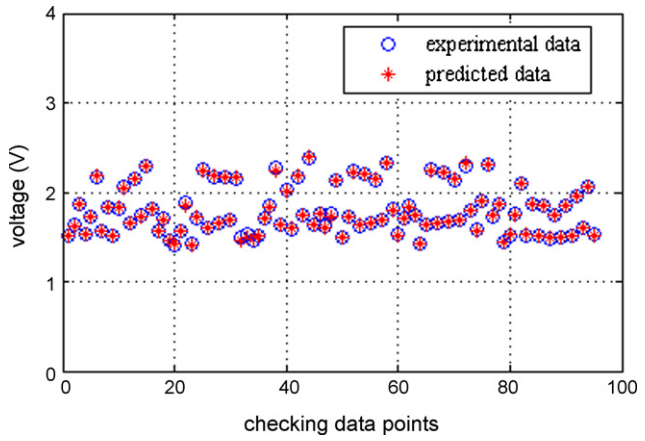

Fig. 9. Comparison of experimental data and predicted voltages using the chosen ANFIS model.

the prediction of performance. ANFIS-based models were tried out with different numbers of the chosen Gaussian curve MFs being assigned with each input variable. It was found that the number of MFs for each of the input variables had a great effect on the model result. The greater the number of MFs for each of the input, the smaller was the RMSE for the training data. However, too many MFs can lead to a large RMSE for the checking data. As Table 2 shows, the training RMSE of the ANFIS (4-4-4) model was 0.01520 which was smaller than that of the ANFIS (3-3-2), while the checking RMSE of the ANFIS (4-4-4) model was much larger than that for the ANFIS (3-3-2). The ANFIS (3-3-2) had better prediction capability than that of ANFIS (4-4-4). The smaller was the checking RMSE, the greater was the generalization capability of the model. It can be concluded that the ANFIS (3-3-2) and ANFIS (4-3-3) are adequate for describing the output of the DMFC due to the smallest value of the checking RMSE and relatively small training RMSE.

It was shown in Table 2 that the ANFIS-based model is better than the ANN and the polynomial. The training and checking RMSE of the ANFIS (4-3-3) model were 0.01781 and 0.03031, respectively. As for ANN, the lowest value of the training RMFS was 0.01906 and for the checking RMSE it was 0.03520. For the polynomial model, the lowest value of the training and checking RMSE increased to 0.03382 and 0.04373, respectively.

Fig. 9 shows the results of the ANFIS-based model compared with the 95 checking data points. Fig. 10 compares the chosen ANFIS model predicted cell voltage with actual experimental values when

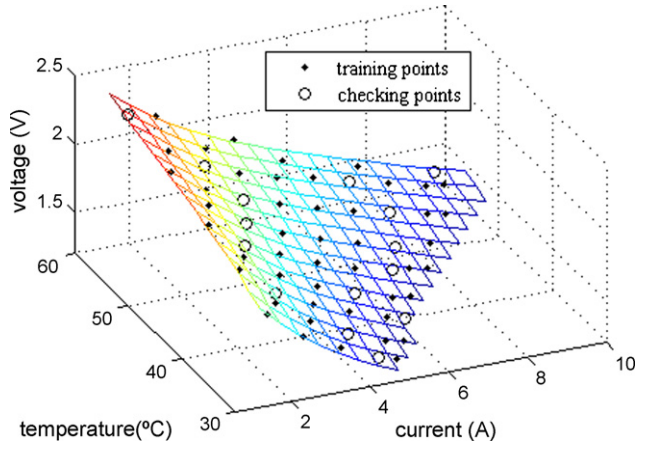

Fig. 10. Comparison of the predicted cell voltage using the chosen ANFIS model with actual experimental values (methanol concentration: 1.00 mol L^{-1}).

Table 3
Fitting parameter numbers and time steps of adaptation

Model	Parameter number	Time steps of adaptation
Polynomial (fifth-order)	56	1
ANN (20 hidden nodes)	120	2600
ANFIS (3-3-2)	90	110

the methanol concentration was 1.00 mol L^{-1}. Figs. 9 and 10 indicate that the results derived from the ANFIS-based model agreed with the experimental data well with no over-fitting taking place on the experimental data.

4.2. Comparison of complexity and running cost

As discussed above, the ANFIS is the best model for describing the cell performance. However, the results presented in Figs. 6–8 indicate that the other two models can simulate the behaviors of the DMFC stack as well. Table 3 lists the numbers of fitting parameters and the time steps of adaptation for those models that are considered to have the highest modeling accuracy and relatively lower complexity.

Obviously, the running cost of polynomial model was the lowest as the LSM was used. It also can be seen from Table 3 that the number of parameters of the polynomial model was smaller than those of the other two models. However, the polynomial model had the worst accuracy.

Also seen in Table 3, the number of parameters for the ANN model (120, with 20 hidden nodes) was only a litter larger than that of the ANFIS-based model (90, 3-3-2), while the training epochs were 2600 versus 110. This shows that the running cost of the ANFIS model is much cheaper than that of the ANN model.

5. Performance analysis based on the obtained ANFIS

After the ANFIS model has been established, the characteristics of the DMFC can be studied based on the obtained ANFIS model. The ANFIS (3-3-2) was taken as the model for detailed study of the DMFC stack.

The contours of the stack voltage at each of the six methanol concentrations are shown in Fig. 11. The stack voltage is interpreted as heights with respect to the concentration–temperature plane. When the concentrations were below 1.67 mol L^{-1}, the performance increased with increase of methanol concentration. However, when the concentration was increased to 1.67 mol L^{-1}, the performance of the DMFC decreased.

Fig. 12 shows the constant concentration surfaces [23] (CCSs) spread out in an ordered manner for concentrations below 1.67 mol L^{-1}. Fig. 13 shows that the CCSs for concentrations 2.00 and 2.33 mol L^{-1} intersect each other, and the CCS for 1.67 mol L^{-1} concentration is above those two surfaces. It indicates that the performance of the DMFC at 1.67 mol L^{-1} is greater than that at 2.00 and 2.33 mol L^{-1}. This is because a higher concentration can reduce the DMFC performance due to the methanol crossover phenomenon [27]. It is concluded that the concentration should not be more than 1.50 mol L^{-1} because a higher concentration can lead to lower fuel utilization efficiency and the lower Faradic efficiency [28–30].

Figs. 11–13 also indicated that the cell performance increased with increase of temperature. We know that high temperature can also intensify methanol crossover which may decrease the efficiency of the system. Thus, in order to obtain higher fuel utilization efficiency, both methanol concentration and temperature should be adjusted according to the load of the system. That is the concentration and temperature should be maintained at suitable low levels

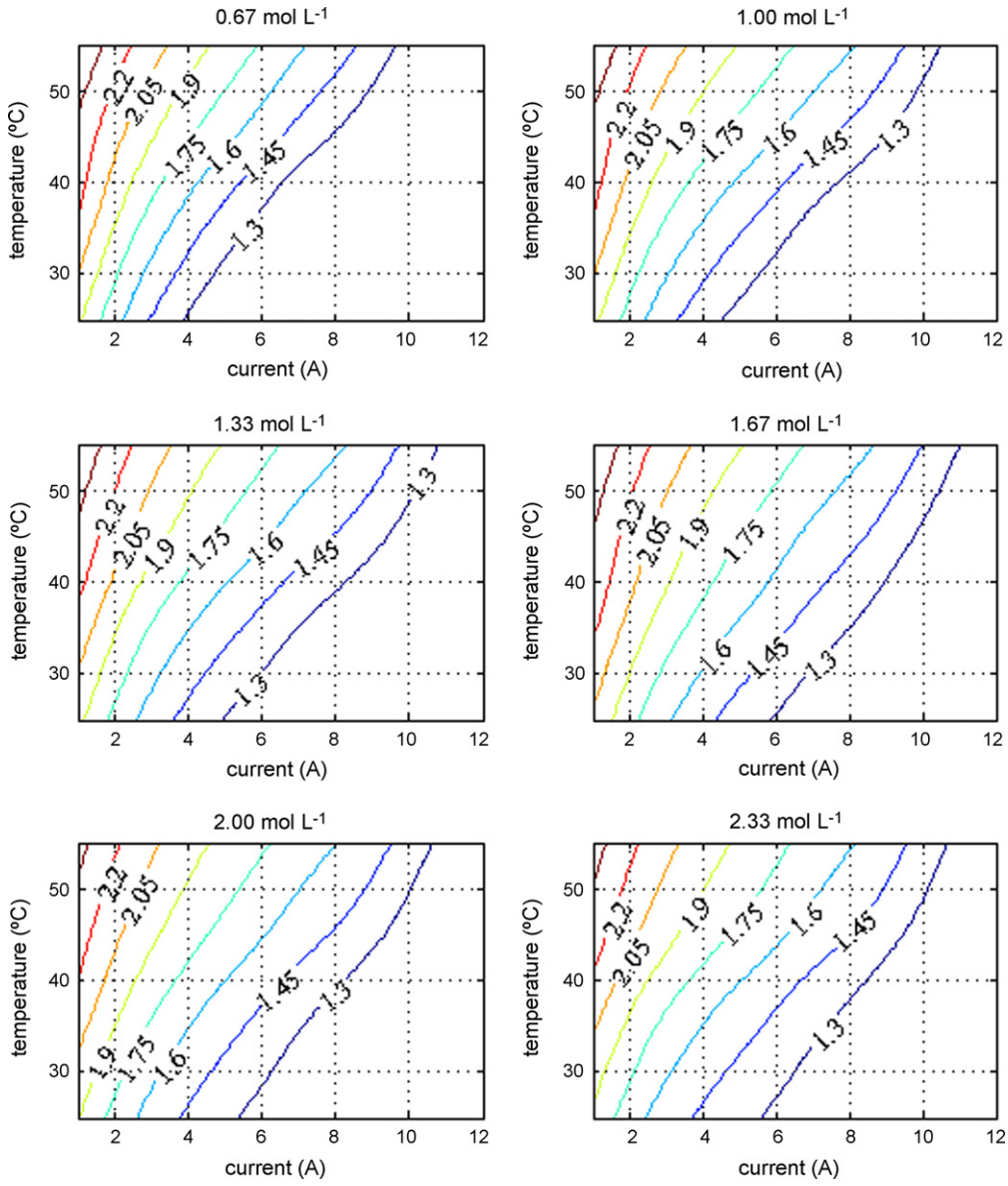

Fig. 11. The contour of the stack voltage for different methanol concentrations (methanol concentration: 0.67, 1.00, 1.33, 1.67, 2.00 and 2.33 mol L^{-1}).

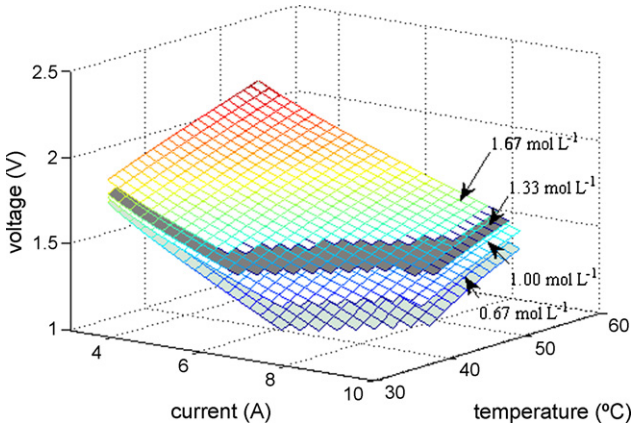

Fig. 12. The constant concentration surfaces for low methanol concentrations (methanol concentration: 0.67, 1.00, 1.33 and 1.67 mol L^{-1}).

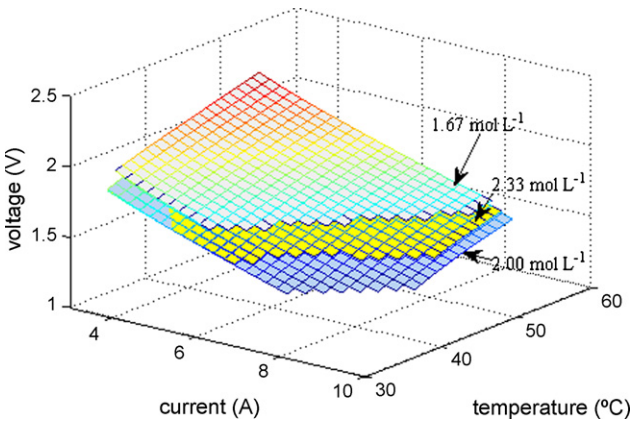

Fig. 13. The constant concentration surfaces for high methanol concentrations (methanol concentration: 1.67, 2.00 and 2.33 mol L^{-1}).

when the system load is small, and only when the load increases should we increase the concentration and temperature.

6. Conclusions

The performance of the DMFC stack was modeled by polynomial, ANN and ANFIS methods. It was found that the three kinds of model could describe the behaviors of the DMFC stack well. Among the three kinds of models, the ANFIS-based model was the best.

Using the ANFIS model, the characteristics of the DMFC were studied. It was shown that temperature and methanol concentration greatly affected the performance of the DMFC. The performance increased with an increase of those factors. Within a limited range of current, the methanol concentrations did not greatly affect the stack voltage. In order to obtain a higher fuel utilization efficiency, the methanol concentration and temperature should be adjusted according to the load on the system. The concentration and temperature should be maintained at suitable lower levels when the system load is small.

In this study, all the experimental data for tuning the models were obtained under steady-state operating conditions. As a matter of fact, a dynamic model is also very important for analyzing and predicting the cell performance [9,10,16,19]. Future work will be focused on developing ANFIS-based model that can describe the cell performance under the dynamic operation conditions, and incorporating other operating parameters into the ANFIS model.

Acknowledgements

The work was funded by the National High Technology R&D Program of China (2006AA05Z138), and Natural Science Foundation of China (50573041 and 50703021). The authors also wish to thank the anonymous reviewers and Dr. Rebing Wu for their valuable comments.

References

[1] C.K. Dyer, J. Power Sources 106 (2002) 31–34.
[2] C. Dyer, Sci. Am. (1999) 88–93.
[3] W. Qian, D.P. Wilkinson, J. Shen, H. Wang, J. Zhang, J. Power Sources 154 (2006) 202–213.
[4] A. Oedegaard, C. Hentschel, J. Power Sources 158 (2006) 177–187.
[5] J.H. Han, H.T. Liu, J. Power Sources 164 (2007) 166–173.
[6] K.T. Jeng, C.W. Chen, J. Power Sources 112 (2002) 367–375.
[7] Z.H. Wang, C.Y. Wang, J. Electrochem. Soc. 150 (4) (2003) 508.
[8] H. Dohle, J. Divisek, R. Jung, J. Power Sources 86 (2000) 469.
[9] S. Jemei, D. Hissel, M.C. Pera, J.M. Kauffmann, J. Power Sources 124 (2) (2003) 479–486.
[10] S.D. Ou, E.K. Luke, Achenie, J. Power Sources 140 (2005) 319–330.
[11] L.X. Wang, IEEE Trans. Automat. Contr. 40 (1995) 11–23.
[12] J. Zhang, IEEE Trans. Fuzzy Syst. 13 (4) (2005) 417–427.
[13] X.K. Su, G.M. Zeng, G.H. Huang, J.B. Li, J. Liang, L.L. Wang, C.Y. Du, Eng. Appl. Artif. Intell. 20 (2007) 239–247.
[14] L. Arafeh, H. Singh, S.K. Putatunda, IEEE Trans. Syst. Man Cybern. 29 (3) (1999) 362–370.
[15] J. Jang, IEEE Trans. Syst. Man Cybern. 23 (3) (1993) 665–685.
[16] L.B. Evgueniy Entchev, Yang, J. Power Sources 170 (2007) 122–129.
[17] G.T. Sun, S. Yan, G. Cao, X. Zhu, J. Zhejiang Univ. Sci. 6 (10) (2005) 1084–1089.
[18] K. Assaleh, M. Al-Rousan, J. Appl. Signal Process. 13 (2005) 2136–2145.
[19] X.J. Wu, X.J. Zhu, G.Y. Cao, H.Y. Tu, Simulat. Model. Pract. Theory 16 (4) (2008) 399–409.
[20] W. Dong, G.Y. Cao, X.J. Zhu, Control Intell. Syst. 32 (2004) 146–153.
[21] Y. Liu, X.F. Xie, Y.M. Shang, R. Li, L. Qi, J.W. Guo, V.K. Mathur, J. Power Sources 1 (164) (2007) 322–327.
[22] J. Larminie, A. Dicks, Fuel Cell Systems Explained, John Wiley and Sons, New York, 2002, pp. 40–53.
[23] Y.J. Chiu, H.C. Lien, J. Power Sources 159 (2006) 1162–1168.
[24] B. Widrow, M.A. Lehr, Proc. IEEE 78 (1990) 1415–1442.
[25] H. Ying, Automatica 34 (12) (1998) 1617–1623.
[26] Fuzzy logic Toolbox, MATLAB™.
[27] P. Costamagna, S. Srinivasan, J. Power Sources 102 (2001) 242–252.
[28] J.G. Liu, T.S. Zhao, R. Chen, C.W. Wong, Electrochem. Commun. 7 (2005) 288–294.
[29] R. Jiang, D. Chu, J. Electrochem. Soc. 151 (2004) 69–76.
[30] H.C. Tu, Y.Y. Wang, C.C. Wan, K.L. Hsueh, J. Power Sources 159 (2006) 1105–1114.